THE TURBULENT BOUNDARY LAYER ON A POROUS PLATE: EXPERIMENTAL HEAT TRANSFER WITH UNIFORM BLOWING AND SUCTION, WITH MODERATELY STRONG ACCELERATION

By

W. H. Thielbahr, W. M. Kays, and R. J. Moffat

Report HMT-11

This study supported
by
The National Science Foundation
NSF GK-2201

and

The National Aeronautics and Space Administration
NGL 05-020-134

Thermosciences Division
Department of Mechanical Engineering
Stanford University
Stanford, California

April 1970

THE TURBULENT BOUNDARY LAYER ON A POROUS PLATE: EXPERIMENTAL HEAT TRANSFER WITH UNIFORM BLOWING AND SUCTION, WITH MODERATELY STRONG ACCELERATION

By

W. H. Thielbahr, W. M. Kays, and R. J. Moffat

Report HMT-11

This study supported
by
The National Science Foundation
NSF GK-2201
and
The National Aeronautics and Space Administration
NGL 05-020-134

Thermosciences Division
Department of Mechanical Engineering
Stanford University
Stanford, California

April 1970

ABSTRACT

Experimental data are presented for heat transfer to the transpired turbulent boundary layer subject to acceleration at constant values of the acceleration parameter, $K = (\nu/U_\infty^2)(dU_\infty/dx)$, of approximately 1.45×10^{-6}. This is a moderately strong acceleration, but not so strong as to result in laminarization of the boundary layer. The results for transpiration fractions, F , of -0.002, 0.0, and +0.0058 are presented in detail in tabular form, and in graphs of Stanton number versus enthalpy thickness Reynolds number. In addition, temperature profiles at several stations are presented. Stanton number results for F = -0.004, +0.002, and +0.004 are also presented, but in graphical form only.

The data were obtained using air as a working fluid, at relatively low velocities, and with temperature differences sufficiently low (approximately $40^\circ F$) so that the influence of temperature-dependent fluid properties is minimal. All data were obtained with the surface maintained at a temperature invariant in the direction of flow.

NOMENCLATURE

English Letter Symbols:

c_f	friction coefficient ($c_f/2 = g_c \tau_w / \rho_\infty U_\infty^2$)
c_p	specific heat at constant pressure
F	blowing fraction ($F = \dot{m}''/(U_\infty \rho_\infty)$)
g_c	proportionality factor in Newton's 2nd Law
H	velocity profile shape factor
i_s	stagnation enthalpy
K	acceleration parameter ($K = (\nu/U_\infty^2) du_\infty/dx$)
$\dot{m}''$	mass flux through wall (positive if flow is into the boundary layer)
P	pressure
P^+	non-dimensional pressure-gradient parameter ($P^+ = -K/(c_f/2)^{3/2}$)
$\dot{q}''$	heat flux normal to free-stream flow direction
Re_H	enthalpy thickness Reynolds number ($Re_H = \Delta_2 U_\infty \rho_\infty / \mu_\infty$)
Re_M	momentum thickness Reynolds number ($Re_M = \delta_2 U_\infty \rho_\infty / \mu_\infty$)
Re_x	integrated x-Reynolds number ($Re_x = \int_0^x (U_\infty \rho_\infty / \mu_\infty) dx$)
St	Stanton number (see Eq. 5)
t	temperature
T	absolute temperature

$\bar{t}$ temperature difference ratio ($\bar{t} = (t-t_\infty)/(t_w-t_\infty)$)

t^+ non-dimensional temperature ($t^+ = \bar{t}\sqrt{c_f/2}/St$)

U_∞ free-stream velocity

u velocity component in x-direction

u^+ non-dimensional velocity ($u^+ = u/(u_\infty\sqrt{c_f/2})$)

v_w^+ a blowing parameter ($v_w^+ = F/\sqrt{c_f/2}$)

x distance measured in direction of flow

y distance measured normal to flow

y^+ non-dimensional distance from wall ($y^+ = yU_\infty\sqrt{c_f/2}/\nu$)

Greek Letter Symbols:

δ_2 momentum thickness of boundary layer

Δ_2 enthalpy thickness of boundary layer (see Eq. (3))

ν kinematic viscosity ($\nu = \mu/\rho$)

μ dynamic viscosity

ρ fluid density

τ shear stress

Subscripts:

w refers to evaluation at the wall, or wall state

∞ refers to evaluation in the free-stream

s refers to stagnation condition

T refers to the state of the transpired fluid before passing through surface plate

INTRODUCTION AND OBJECTIVES

This paper is one of a series on momentum and heat transfer processes involving the transpired turbulent boundary layer. All of these papers are based on data obtained as part of a systematic experimental investigation employing the Stanford Heat and Mass Transfer Apparatus.

The first two papers in this series, Moffat and Kays [1], and Simpson, Moffat, and Kays [2], covered the heat transfer and hydrodynamics for constant free-stream velocity, and constant surface temperature, with a range of constant blowing and suction fractions from "blow-off" to asymptotic suction. Whitten, Moffat, and Kays [3] again considered heat transfer, using a constant free-stream velocity, but included the influence of both blowing fraction and surface temperature varying in the main flow direction. Simpson, Whitten, and Moffat [4] is a study of turbulent Prandtl numbers extracted from the data of the first two papers.

A second phase of the program has been concerned with the influence of free-stream acceleration on both the momentum and heat transfer characteristics of the transpired turbulent boundary layer. The first paper in this phase, Kays, Moffat, and Thielbahr [5], is specifically concerned with the phenomena described as "laminarization" in an accelerated transpired turbulent boundary layer, and also with a finite-difference prediction technique that adequately predicts the effects of strong accelerations, and predicts virtually all of the results in the preceding papers. Kays, Moffat, and Thielbahr contains samples of the experimental data obtained during the acceleration phase

of the program, but since these data are only used to support a discussion and analysis of the "laminarization" phenomena, they are not presented in sufficient detail to be useful to other workers. The primary objective of the present paper, as well as that of a companion paper, Julien, Kays, and Moffat [6], is to present and document some selected experimental data, obtained under a moderately strong free-stream acceleration, in sufficient detail and with all of the experimental conditions sufficiently described, so that other workers can make meaningful comparisons with data and theoretical prediction techniques. Julien, Kays, and Moffat [6] is confined to the momentum boundary layer alone, while the present paper is concerned with the development of the thermal boundary layer. No theoretical analysis is presented in either case; the purpose of these papers is to present facts and data that can be used to test the validity of new theories.

Specifically, the objectives of the present paper are:

1. To present Stanton number data taken under conditions of constant surface temperature, for three transpiration rates: ($F = -0.002, 0.0, +0.0058$) for one case of moderately strong constant K acceleration, $K = 1.47 \times 10^{-6}$, including the constant velocity recovery region following the acceleration, and the constant velocity region before acceleration.

2. To present a series of temperature profiles taken simultaneously with the Stanton number data, covering the same range of conditions.

THE ASYMPTOTIC BOUNDARY LAYER

The acceleration parameter $K\left(K = \frac{\nu}{U_\infty^2}\frac{dU_\infty}{dx}\right)$ is a convenient measure of the strength of an imposed pressure gradient. This parameter appears explicitly in a particular form of the two-dimensional, integral momentum equation,

$$\frac{dRe_M}{dRe_x} = c_f/2 - Re_M(1 + H)K + F \qquad (1)$$

Examination of Eq. (1) reveals that if K is positive and constant, and F constant, the term dRe_M/dRe_x can vanish if c_f, Re_M and H reach appropriate values. A boundary layer having a constant momentum thickness Reynolds number will be called an "asymptotic" boundary layer. This particular type of boundary layer is characterized by constant Re_M, K (positive), and F. Furthermore, if the hydrodynamic profiles were completely similar, then H and c_f would also be constant. Under these conditions, the important inner region variables P^+ and v_w^+ remain constant.

Exact solutions to the asymptotic laminar boundary layer are available [7]. Townsend [8] considered an exactly self-preserving turbulent boundary layer with constant, positive K, and showed it possessing a constant Re_M. Launder and Stinchcombe [9] established a turbulent boundary layer at a constant value of K, and obtained near-constant Re_M, c_f, and H.

Because so many parameters remain constant, the asymptotic boundary layer provides a particularly convenient configuration for study of accelerated boundary layers. Although the overall

experimental program covered a range of values of K, the present paper is restricted to $K \approx 1.45 \times 10^{-6}$. In addition, all runs were restricted to constant blowing fraction (F) and constant surface temperature (t_o) boundary conditions. The blowing fraction ranges from $-0.004 \leq F \leq +0.006$. This range of F is of practical interest since the upper limit is near blow-off ($F \approx +0.010$), and asymptotic suction conditions (where $St = -F$) are rapidly approached at $F = -0.004$.

EXPERIMENTAL APPARATUS

All data were taken on the Stanford Heat and Mass Transfer Apparatus. This apparatus provides the capability of accurately evaluating heat transfer coefficients along a flat surface in the presence of (1) arbitrary free-stream velocity distribution, (2) arbitrary surface transpiration (blowing or suction), and (3) arbitrary surface temperature distribution. The working fluid is air.

A detailed description of the apparatus can be found in reference [1]. Briefly, the test section is a rectangular flow duct eight feet long by twenty inches wide by six inches high (at the air free-stream entrance). Twenty-four porous bronze plates form the lower surface, two stationary plexiglass walls form the sides, and a flexible plexiglass top provides the means to produce any desired variation in free-stream velocity. All data were taken on the center six-inch span of each porous segment. The main air system is supplied by a 2000 scfm blower which can produce up to 44 ft/sec free-stream velocity at the duct entrance.

The transpiration air system provides individual control of flow through each of the twenty-four porous plates. The plates are electrically heated so the system can operate with no surface mass transfer. The transpiration system also has the capability for simultaneous blowing and suction through different plates.

Each porous plate is 0.25 inches thick, sintered together from spherical bronze particles (0.002 to 0.007 inches diameter). The surface has an RMS roughness of 50-200 microinches (measured with 0.0005 inch radius stylus), and the plate is uniformly porous ($\pm$ 6%) over the center six inch span. Each plate is heated individually by electrical energy dissipated from 0.012 inch diameter wires glued into grooves on the back of the plate. The spacing of the wires was selected to yield negligible temperature variation across the plate surface. Each plate's surface temperature is determined from an average of five iron-constantan thermocouples imbedded in the plate at a depth of 0.040 inches from the free-stream surface.

Acceleration of the main stream is necessarily accompanied by a gradient in static pressure in the flow direction. This gradient acts to cause the transpiration flow thru each segment to be higher than average on the downstream edge and lower than average on the upstream edge. The maximum disturbance in transpiration flow necessarily occurs on the last plate in the accelerating region, where the local value of $\frac{dP}{dx}$ is largest. The combination of strong acceleration (high K) and low blowing fraction produces the largest percent variations in the transpired flow. Under these conditions ($K = 1.45 \times 10^{-6}$, $F = +0.001$) the

transpiration flow at the upstream and downstream edges of the worst plate differed by 5%.

The streamwise static pressure distribution along the test section was obtained from forty-eight equally spaced pressure taps located on one of the side walls. Free-stream velocity distribution, and the axial distribution of K, were calculated from Bernoulli's equation. It was confirmed experimentally that wall static pressure taps located one-inch above the porous plates adequately measure the local static pressure in the center of the duct: i.e., there were no significant lateral or vertical gradients in static pressure in the potential core for $0 \leq K \leq 1.45 \times 10^{-6}$, in the region of the boundary layer.

All stagnation pressures were measured with flattened mouth pitot probes, approximately 0.015 inches high by 0.040 wide. A description of these probes and application of the appropriate corrections can be found in references [2] and [11]. The boundary layer temperature probe consisted of an iron-constantan thermocouple with the junction flattened to a height of 0.009 inches. Electrical continuity was used to establish the location of contact between wall and probe. A one-inch displacement micrometer, having a least count of 0.001 inch, provided the means of measuring vertical displacement.

A uniform hydrodynamic and energy potential flow core existed on all test runs. Tests with a constant temperature hot wire anemometer established a maximum turbulence intensity of 1.2% at an entrance free-stream velocity of 44 ft/sec. For the tests at entrance velocity of 25 ft/sec, the lowest free-stream

velocity used, the free-stream turbulence intensity was reduced to 0.8% with the addition of a special set of flow screens.

To achieve constant K flow at F = 0 , the flexible upper wall was bent downward at a constant slope. When uniform blowing is present, a constant sloped upper wall still provides a reasonably constant K flow.

For a fixed inlet velocity, large values of K are achieved at the expense of testing length. Thirty-two inches of test surface were exposed to the maximum K achieved in this study (1.45×10^{-6}). K varied from its initial level (K = 0) to its maximum in about 1.4 feet, and after acceleration recovered to K = 0 in about 1.0 feet.

When Re_M at the start of acceleration was approximately equal to the anticipated asymptotic Re_M , the flow adjusted to its asymptotic condition in a relatively small distance. It was not always possible to achieve this condition; the largest percent deviations from the asymptotic condition were associated with the higher suction runs.

WALL HEAT FLUX AND QUALIFICATION TESTS

The surface heat flux, $\dot{q}''_w$, was calculated from an energy balance performed on a control volume covering the center six inches of porous plate. Applying the 1st Law of Thermodynamics to the control volume yields,

$$\dot{q}''_w = \text{electric power} - \text{losses} - \dot{m}''(i_{s,w} - i_T) \qquad (2)$$

Description of the various losses can be found in reference [1].

To qualify the test rig, a series of energy balance tests were performed before and after these tests. These tests are routinely conducted every six months to confirm the validity of the thermal model. The test procedures are documented in reference [1]. The energy balance tests do not utilize main-stream flow; the top cover is removed so as to provide one-dimensional flow of transpired fluid. Under these conditions $\dot{q}''_w = 0$ thus enabling the individual energy transfer mechanisms in Eq. (2) to be properly evaluated for each plate. Upon completion of these tests, it was concluded that no significant change in the characteristics of the apparatus had occurred during the course of these tests.

Based on the method of Kline and McClintock [10], the calculated uncertainty in Stanton number was $\pm$ 0.0001 for all but the high suction runs (F = -0.002 and -0.004). At these higher suction fractions, the St uncertainty interval rose to +0.0002. The uncertainty in enthalpy thickness Reynolds number (calculated from the two-dimensional energy integral equation) averaged approximately 2% of the reported value for all but the higher suction runs. Uncertainties in the acceleration parameter K ranged from 8% to 17% of the reported values. For a discussion of the uncertainties in c_f, see reference [11], or reference [6].

ROUGHNESS AND TWO-DIMENSIONALITY

The RMS roughness of the plate surfaces varied between 50 and 200 microinches, measured with a half-mil stylus. Roughness effects on $c_f/2$ and St can probably be discounted if this

roughness is small compared to the thickness of the effective laminar sublayer.

Assuming the sublayer for an impermeable, flat plate flow to extend to $y^+ = 5$, this represents a physical thickness of 0.0015 inches when $Re_M = 500$ and $U_\infty = 125$ ft/sec, well beyond the 0.0002 inch maximum roughness. All impermeable flat plate data reported here are for conditions which are conservative compared to these conditions.

The effects of surface roughness have not been established for blown and sucked layers, but Simpson [2] and others have shown that the sublayer thickness decreases with blowing while the data reported here show that acceleration tends to thicken the sublayer. The most critical conditions, therefore, would be those in the recovery region: i.e., with no acceleration, with a high blowing fraction, and with a high free stream velocity.

Data were taken at $F = +0.006$ and $U_\infty = 75$ ft/sec in the recovery region following a strong acceleration. Even under these conditions the value of skin friction was such that the viscous sublayer extended at least to $y = 0.001$ (assuming a critical y^+ of 1.0) which again seems safe.

Velocity profile and heat transfer data were taken at constant free-stream velocities of 42, 86 and 126 ft/second with no blowing. The resulting values of friction factor and Stanton number, and the $u^+ - y^+$ profiles agreed with accepted standards for the 42 and for the 86 ft/second data. The friction factor was about 8% high for the 126 ft/second data, and the $u^+ - y^+$ profiles showed a shift to a lower value of the constant (to a

value of 4.0). All of the tabular data reported here are for velocities less than 75 ft/second and, consequently, are felt to be free of roughness effects.

Two dimensionality of a boundary layer flow can be established only by elaborate and precise traversing of the boundary layer. This was not done in the present tests, but there is strong secondary evidence that the flow was acceptably two-dimensional. First, the spanwise variation of momentum thickness, across the center 6-inch span, was on the order of 6%-8% which precludes any major cross flows. Second, and most important, is the evidence available from energy balance considerations applied to the boundary layer.

The local enthalpy thickness, Δ_2, was calculated from its definition,

$$\Delta_2 = \frac{\int_0^x \rho u (i_s - i_{s,\infty}) dy}{\rho_\infty U_\infty (i_{s,w} - i_{s,\infty})} \qquad (3)$$

and from the two-dimensional energy integral equation with constant surface temperature,

$$St + F = \frac{d\Delta_2}{dx} + \Delta_2 \left(\frac{1}{U_\infty} \frac{dU_\infty}{dx} + \frac{1}{\rho_\infty} \frac{d\rho_\infty}{dx} \right) \qquad (4)$$

The velocity profiles of Julien [11] (also summarized in Julien, Kays, and Moffat [6]), taken under identical free stream and blowing fraction operating conditions on the same apparatus,

and the measured temperature profiles, were used to calculate Δ_2 from Eq. (3). Experimental St , U_∞ , and F were utilized in Eq. (4) to calculate Δ_2 .

The uncertainty in Δ_2 from Eq. (3) ranged from 3% to 8% for $F \geq -0.001$. Uncertainty in Δ_2 from Eq. (4) ranged from 2% to 6% for $F \geq -0.001$. It was concluded for $F \geq -0.001$ that when Δ_2 from Eq. (3) was within 8% of Δ_2 calculated from Eq. (4), the boundary layer development along the test surface was sufficiently two-dimensional. Excluding the first temperature profile, that being in the constant U_∞ region preceding acceleration, all data for $F \geq -0.001$ met this two-dimensionality criterion.

The uncertainty in Δ_2 from equations (3) and (4) became greater than 10% for $F = -0.002$. This large uncertainty means that this method is unsatisfactory for checking two-dimensionality for those conditions. All zero pressure gradient, flat-plate skin friction and heat transfer data corresponding to $F = -0.002$ agreed with the two-dimensional data of references [1] and [2].

Conclusions regarding two-dimensionality of the flow are as follows:

1. The pressure gradient and recovery section data describe the characteristics of a nearly two-dimensional turbulent boundary layer.

2. Prior to acceleration, the experimental Stanton numbers obeyed an accepted smooth wall, two-dimensional correlation within $\pm 5\%$.

DETERMINATION OF BOUNDARY LAYER INTEGRAL DESCRIPTORS

Boundary layer enthalpy thicknesses were calculated from temperature and velocity profile data as well as from integration of the two dimensional energy integral equation along the plate surface. Neither a radiation nor a turbulent fluctuation correction was applied to the indicated probe temperatures. Errors induced as a result of "wall effects" were assumed negligible. The length of bare thermocouple wire exposed to the flow was selected to reduce the conduction loss from the junction. It was assumed that the indicated probe temperature corresponded to the y-position of the probe's half-height. The uncertainty in y-position was assumed to be ± 0.001 inch. Local velocities were low enough so as to yield no significant difference between local "adiabatic probe" and stagnation temperatures.

In the wall dominated region of the boundary layer, $t^+ - y^+$ coordinates are appropriate. The t^+ and y^+ variables were evaluated using free-stream fluid properties. The Stanton number contained in the definition of t^+ was corrected to constant properties, employing the assumption that the heat transfer coefficient varies as the negative 0.4 power of (T_w/T_∞). The skin friction coefficient, obtained from reference [11], corresponds to approximately the same free-stream conditions.

The velocity profile data were taken in separate isothermal tests, see reference [11], or reference [6], and not during the heat transfer tests. An experimental and analytical study was undertaken to find the most accurate method of combining isothermal

hydrodynamic profile data with temperature profile data from the heat transfer case so as to calculate local δ_2 and Δ_2 [12]. From this study it was concluded that if the free-stream conditions are similar for the isothermal and nonisothermal cases, a good approximation to apply in calculating δ_2 with heat transfer is $\left(\frac{u}{U_\infty}\right)_H = \left(\frac{u}{U_\infty}\right)_I$, where $(\ )_H$ and $(\ )_I$ subscript notation designate heat transfer and isothermal situations, respectively. This same relationship can also be used in the evaluation of Δ_2. These results apply when $0.95 \leq \frac{T_\infty}{T_W} \leq 1.05$, and were verified by experiments conducted with blowing and favorable pressure gradient. For the range of experimental conditions reported in this paper, the error in δ_2 and Δ_2 resulting from this approximation is on the order of 1%.

Local Stanton number was calculated from its definition,

$$St = \frac{\dot{q}''_W}{\rho_\infty U_\infty (i_{s,W} - i_{s,\infty})} \tag{5}$$

As presented in the tables, it has <u>not</u> been corrected for the influence of the 35-40°F temperature differences existing between free-stream and the wall surfaces.

The reported values of Re_H were calculated by integration of the two-dimensional energy integral equation (constant t_o),

$$\frac{dRe_H}{dRe_x} = St + F \tag{6}$$

starting with an estimate of the enthalpy thickness at the beginning of the heated plate. An exception to this procedure is at the points where temperature and velocity traverses were made, and were Eq. (3) was used to evaluate Δ_2. Thus an idea of the uncertainty in the reported values of Re_H can be had by comparing the results of two completely independent procedures.

EXPERIMENTAL RESULTS

The heat transfer data reported here are taken from the larger program reported by Thielbahr [12] covering accelerations at $K = 0.55, 0.75,$ and 1.45×10^{-6}. The tabular and graphical results presented here should suffice to describe the principal effects of acceleration within this range. A prediction program which properly handles the impermeable flat plate case, the earlier results of Moffat and Kays [1], and the conditions reported here will, in all probability, adequately predict all the intermediate data.

The experimental results for one value of the acceleration parameter, $K = 1.45 \times 10^{-6}$, and three values of the blowing fraction, $F = -0.002$, 0.0, and $+0.0058$, are presented in tabular form in Tables 1 and 2. The same data are shown graphically in Figs. 1-5, but in addition Stanton number data is presented in Figs. 1 and 2 for $F = +0.004, +0.002,$ and -0.004.

In Table 1, Stanton numbers are presented, for each of the three runs considered, as a function of axial position along the test plate beginning with plate #3. The Stanton numbers are

averages over a 4-inch plate, but are presented as local Stanton numbers at x-distances which are measured from the beginning of the first plate to the centerline of the indicated plate. An exception to this rule is the case of the positions for which $c_f/2$ is indicated. These are positions at which temperature and velocity profiles have been taken, and the local Stanton number for each of these positions has been estimated by interpolating on a smooth curve through the data at the plate centerlines.

For each of the three tabulated runs, there is an approach section for which $K = 0$, and the first of the velocity and temperature profiles are taken in this section. Three (and in one case, four) profiles are taken in the acceleration region, and then three (or two) in the recovery region following acceleration. The enthalpy thickness Reynolds numbers, Re_H, obtained from the temperature and velocity profiles are indicated by (*); all other values of Re_H are obtained by integration of Eq. (6). A comparison of the values of Re_H obtained by the two methods provides an indication of the uncertainty in Reynolds number.

Note that the momentum thickness Reynolds numbers, Re_M, appear to approach a constant value in the accelerated region, as is suggested by Eq. (1). This is particularly noticed in the run for $F = +0.0058$, where the anticipated asymptotic Reynolds number is closely approached just before acceleration starts. For the other two runs, the approach Reynolds number considerably

exceeds the apparent asymptotic value, with the result that there is a continuous decrease in Reynolds number during acceleration. After acceleration, Re_M in all cases increases. Note that Re_H continuously increases in all cases before, during, and after acceleration. This is consistent with Eq. (6), which unlike the analogous Eq. (1), does not contain an explicit acceleration term. However, Eq. (6) does indicate the possibility of a constant Re_H boundary layer when F is negative (suction) so that $St = -F$. An example of this, which will occur whether there is acceleration or not, will be shown in the Figures.

In Table 2, all of the temperature profiles indicated in Table 1 are presented in detail. At each position the normal distance y is given, along with the non-dimensional y^+ and t^+. Additionally, at the first station for each run, $x = 13.78$ in., u/U_∞ and $\overline{t}$ are given so that those desiring to test theoretical models in thermal boundary layer prediction schemes have all of the necessary data to start calculations at $x = 13.78$ in.

Figs. 1 and 2 show plots of Stanton number as a function of Re_H for six different values of F, including the three values of F given in the Tables. The open data points are those for which Re_H has been evaluated by integration of Eq. (6); the filled-in data points differ only in that Re_H is evaluated from the temperature and velocity profiles, and Eq. (3). The dashed lines are the results of Moffat and Kays [1] for transpiration with constant free-stream velocity.

Most of the heat transfer characteristics of the transpired and accelerated turbulent boundary layer can be seen in the data on these figures. For $F = 0$, Fig. 1, acceleration causes a decrease in Stanton number below the expected value for constant U_∞. This decrease is caused primarily by an increase in the viscous sublayer thickness, as is discussed in reference [5]. Higher values of K cause a more pronounced decrease, and if K is sufficiently high, the boundary layer will apparently revert to a completely laminar one. However, at $K = 1.45 \times 10^{-6}$ there is no evidence of "laminarization".

Following acceleration, there is an abrupt increase in Stanton number as the sublayer returns to its zero-pressure-gradient condition, but now the thermal boundary layer is thicker than the momentum boundary layer (see comparison of Re_H and Re_M in Table 1), and the return to the constant U_∞ value of Stanton number is not complete. The recovery is rather slow, but this is predictable from the integral equation; Eqs. (1) and (6). Recovery will not be complete until Re_M has closely approached its usual relationship to Re_H.

The results for blowing, $F = +0.004$ on Fig. 1, and $F = +0.002$ and $+0.0058$ on Fig. 2, do not show a dip in Stanton number with acceleration; in fact for $F = +0.0058$ there is actually an increase in Stanton number when acceleration is applied. Blowing alone causes a very substantial drop in friction coefficient, and in Stanton number, caused primarily by the influence of transpiration on the shear stress and heat flux

distribution in the region near the wall. This effect can be readily seen if the region near the wall is approximated as a Couette flow, and the resulting equations for shear stress and heat flux are examined.

$$\tau/\tau_w = 1 + v_w^+ u^+ + P^+ y^+ \qquad (7)$$

$$\dot{q}''/\dot{q}_w'' = 1 + v_w^+ u^+ \qquad (8)$$

Blowing also causes a decrease in the viscous sublayer thickness, but this is much more than offset by the shear stress and heat flux effect. Acceleration causes an opposite effect on shear stress distribution from that caused by blowing (note in Eq. (7) that acceleration corresponds to negative P^+), resulting in an increase in friction coefficient (see Table 1 for $F = +0.0058$). There is no directly analogous effect on heat flux distribution (see Eq. (8)), but heat flux distribution is indirectly affected by the newly established velocity distribution. The result is that Stanton number responds as does the friction coefficient, although not so markedly, and partly regains what it has lost as a result of blowing alone. Acceleration also causes an increase in the viscous sublayer thickness, as is the case for no transpiration, but this effect is evidently more than offset by the shear stress effect when the blowing fraction is large.

Suction alone results in an increase in Stanton number and friction coefficient, due again to the influence of transpiration on the heat flux and shear stress distribution. In this case, however, acceleration has a very strong effect on Stanton number, see Fig. 2 for example, while the effect on $c_f/2$ is slight,

see Table 1. Suction causes a thickening of the viscous sublayer, and acceleration further thickens it, instead of opposing as is the case for blowing and acceleration. The substantial decrease in Stanton number caused by acceleration of a sucked boundary layer is believed to be primarily the viscous sublayer effect.

It is interesting to note the limitation imposed by the energy integral equation, Eq. (6), on the suction heat transfer behavior. If the sucked gas is at plate temperature when it reaches the plate surface, the suction limit is reached so that $St = -F$. For the case of $F = -0.002$ on Fig. 2, the suction limit is almost reached in the accelerated region. For the case of $F = -0.00395$ on Fig. 1, the suction limit is actually attained, and the cluster of data points around $St = 0.004$ is an indication of a constant value of Re_H and St and the random experimental uncertainty. It appears that Re_H is decreasing in the accelerated region, but since Re_H is determined by integration of Eq. (6), the error in Re_H is cumulative. Temperature profiles were not taken for this run. It is apparent that the suction limit for this run would have been reached without acceleration at about $Re_H = 640$. Acceleration, by decreasing Stanton number, merely hastens the attainment of the suction limit.

The temperature profiles, Figs. 3, 4, and 5, substantially corroborate the explanation given above in connection with the Stanton number behavior. The various effects are probably seen most clearly in Fig. 4 for $F = 0.0$. In the inner region, $y^+ < 100$, the t^+, y^+ behavior is virtually identical both before and after acceleration. During acceleration the inner region data

is again virtually identical out to y^+ equal 30 or 40, but t^+ in this region is very substantially higher than for no acceleration. This, along with the same behavior in u^+, y^+ plots, can be discussed in terms of a thicker sublayer during acceleration. It can also be seen on this plot that the behavior in the recovery region following acceleration is almost entirely an outer region effect, the inner region having quickly recovered.

In the strongly blown run, Fig. 5, similar viscous sublayer effects are present, but they make a relatively smaller contribution to overall behavior. Quite the reverse is true for suction, Fig. 3.

SUMMARY AND CONCLUSIONS

In this paper experimental data have been presented for heat transfer to transpired turbulent boundary layers subjected to moderately strong accelerations in which the acceleration parameter, K, has been maintained approximately constant at a value of 1.45×10^{-6}. Various constant transpiration fractions from -0.004 to +0.0058 have been considered. All data were obtained with a uniform surface temperature in the flow direction. Sufficient documentation has been provided to establish the precision of the data, and to allow meaningful comparisons with boundary layer prediction techniques.

It has been shown that acceleration can be interpreted as causing an increase in the viscous sublayer thickness, which has

a very substantial influence on heat transfer behavior for suction, a moderate effect for no transpiration, and very little effect for strong blowing. The boundary layers remained turbulent in character for the acceleration considered, $K = 1.45 \times 10^{-6}$.

For suction, and for no blowing, acceleration causes a decrease in Stanton number below the value which would obtain at the same enthalpy thickness Reynolds number without acceleration. With blowing, however, this decrease is not noted, and in fact acceleration of a highly blown boundary layer will actually cause an increase in Stanton number. A qualitative explanation for this behavior is presented.

In the region following an acceleration, the inner region (i.e., the viscous sublayer) recovers rapidly to its equilibrium conditions for no pressure gradient, but the outer region recovers rather slowly, apparently because during acceleration the thermal boundary layer has grown substantially relative to the momentum boundary layer.

ACKNOWLEDGEMENTS

This work was made possible by support of the National Aeronautics and Space Administration, NASA Grant NGL 05-020-134, and the National Science Foundation, NSF GK-2201. The continued interest of Dr. Royal E. Rostenbach of NSF and Dr. Robert W. Graham of NASA Lewis Laboratories is greatly appreciated.

REFERENCES

1. Moffat, R. J., and Kays, W. M., "The Turbulent Boundary Layer on a Porous Plate: Experimental Heat Transfer With Uniform Blowing and Suction," Int. Jn. of Heat and Mass Transfer, Vol. 11, No. 10, (1968) pp. 1547-1566.

2. Simpson, R. L., Moffat, R. J., and Kays, W. M., "The Turbulent Boundary Layer on a Porous Plate: Experimental Skin Friction With Variable Injection and Suction," Int. Jn. of Heat and Mass Transfer, Vol. 12, No. 7, (1969) pp. 771-789.

3. Whitten, D. G., Moffat, R. J., and Kays, W. M., "Heat Transfer to a Turbulent Boundary Layer With Non-Uniform Blowing and Surface Temperature," ASME Paper No. 69-IC-168. Accepted for presentation at the Fourth International Heat Transfer Conference, Paris, France, August 31, 1970 to September 5, 1970.

4. Simpson, R. L., Whitten, D. G., and Moffat, R. J., "An Experimental Study of the Turbulent Prandtl Number of Air With Injection and Suction," Int. Jn. of Heat and Mass Transfer, Vol. 13, No. 1, pp. 125-143 (1970).

5. Kays, W. M., Moffat, R. J., and Thielbahr, W. H., "Heat Transfer to the Highly Accelerated Turbulent Boundary Layer With and Without Mass Addition," ASME Paper No. 69-HT-53. Accepted for publication in the Jn. of Heat Transfer.

6. Julien, H. L., Kays, W. M., and Moffat, R. J., "Experimental Hydrodynamics of the Accelerated Turbulent Boundary Layer With and Without Mass Injection," Department of Mechanical Engineering, Stanford University, Stanford, California (1970).

7. Schlichting, H., Boundary Layer Theory, McGraw-Hill Book Co. (1960).

8. Townsend, A. A., The Structure of Turbulent Shear Flow, Cambridge University Press (1956).

9. Launder, B. E., and Stinchcombe, H. S., "Non-Normal Similar Turbulent Boundary Layers." Report TWF/TN/21, Mechanical Engineering Department, Imperial College of Science and Technology, London (1967).

10. Kline, S. J., and McClintock, F. A., "Describing Uncertainties in Single Sample Experiments," Mechanical Engineering, 75, 1953, 3-8.

11. Julien, H. L., "The Turbulent Boundary Layer on a Porous Plate: Experimental Study of the Effects of a Favorable Pressure Gradient," Ph.D. thesis, Department of Mechanical Engineering, Stanford University, Stanford, California (1969). Available from University Microfilms, Ann Arbor, Michigan.

12. Thielbahr, W. H., "The Turbulent Boundary Layer: Experimental Heat Transfer With Blowing, Suction, and Favorable Pressure Gradient," Ph.D. thesis, Department of Mechanical Engineering, Stanford University, Stanford, California (1969). Available from University Microfilms, Ann Arbor, Michigan.

TABLE 1

STANTON NUMBER RESULTS AND INTEGRAL PARAMETERS

Run No. 080668-1

$K = 1.47 \times 10^{-6}$ nominal

$F = -0.002 \pm 0.00003$

$t_\infty = 66.7 \pm 0.5^\circ F$, $t_w = 102.2 \pm 0.8^\circ F$

P = 29.85 in Hg at exit

X,in	U_∞,ft/sec	$Kx10^6$	Re_H	Re_M	$c_f/2$	St
10	25.0	-0.03	396			0.00384
13.78	24.9	0.00	543*	656	0.00353	0.00369
14	24.9	-0.02	487			0.00369
18	25.0	0.37	570			0.00355
22	25.9	0.92	648			0.00345
26	27.7	1.38	721			0.00319
29.67	29.9	1.41	811*	600	0.00340	0.00304
30	30.2	1.44	787			0.00303
34	33.2	1.56	848			0.00284
37.69	36.7	1.42	963*	486	0.00330	0.00271
38	36.9	1.40	902			0.00270
42	41.5	1.51	955			0.00260
45.64	46.9	1.53	1056*	392	0.00323	0.00246
46	47.5	1.52	1000			0.00245
49.63	54.9	1.51	1073*	349	0.00310	0.00242
50	55.7	1.48	1050			0.00242
54	66.0	0.80	1080			0.00222
58	67.8	0.00	1110			0.00216
61.77	67.7	0.01	1116*	421	0.00315	0.00252
62	67.7	-0.01	1160			0.00251
66	67.8	0.01	1250			0.00282
69.70	67.8	0.01	1293*	661	0.00330	0.00301
70	67.8	-0.01	1380			0.00302
74	67.8	-0.01	1520			0.00292
78	67.7	0.00	1650			0.00290
82	67.7	0.00	1770			0.00282
85.78	67.7	0.00	1675*	1130	0.00290	0.00282
86	67.7	0.00	1880			0.00282
90	67.7	0.02	2000			0.00281

*Evaluated from temperature and velocity profiles. All others from integral energy equation.

Run No. 072968-1

$K = 1.47 \times 10^{-6}$ nominal

F = 0.0

$t_\infty = 66.8 \pm 0.5^\circ F$, $t_w = 109.8 \pm 0.6^\circ F$

P = 29.82 in Hg at exit

X,in	U_∞,ft/sec	$Kx10^6$	Re_H	Re_M	$c_f/2$	St
10	24.8	-0.11	525			0.00313
13.78	24.7	0.02	727*	881	0.00230	0.00293
14	24.7	0.04	678			0.00292
18	24.9	0.43	822			0.00276
22	26.0	1.14	961			0.00260
26	28.0	1.47	1100			0.00238
29.67	30.3	1.38	1243*	905	0.00245	0.00224
30	30.5	1.47	1240			0.00224
34	33.7	1.51	1380			0.00213
37.69	37.2	1.44	1537*	796	0.00252	0.00206
38	37.5	1.47	1530			0.00206
42	42.2	1.47	1690			0.00200
45.64	47.8	1.45	1898*	747	0.00248	0.00197
46	48.4	1.51	1880			0.00197
50	57.0	1.49	2080			0.00188
54	67.8	0.80	2320			0.00182
58	69.6	-0.01	2580			0.00191
61.77	69.6	0.01	2795*	1234	0.00222	0.00183
62	69.6	-0.01	2850			0.00183
66	69.6	0.02	3110			0.00183
69.70	69.7	0.00	3280*	1793	0.00191	0.00178
70	69.7	0.00	3360			0.00179
74	69.8	0.00	3610			0.00175
78	69.8	0.01	3860			0.00173
82	70.0	0.02	4100			0.00169
85.78	70.1	0.00	4266*	2760	0.00175	0.00169
86	70.1	0.00	4350			0.00169
90	70.1	0.00	4590			0.00169

Run No. 082768-1

$K = 1.45 \times 10^{-6}$ nominal

$F = +0.0058 \pm 0.00006$

$t_\infty = 67.6 \pm 0.8^\circ F$, $t_w = 98.8 \pm 1.3^\circ F$

P = 30.87 in Hg at exit

X,in	U_∞,ft/sec	$Kx10^6$	Re_H	Re_M	$c_f/2$	St
10	25.0	0.00	1050			0.00122
13.78	25.0	0.06	1481*	1676	0.00082	0.00104
14	25.0	0.11	1420			0.00103
18	25.4	0.47	1780			0.00088
22	26.4	1.02	2140			0.00083
26	28.4	1.34	2530			0.00093
29.67	30.8	1.39	2924*	2019	0.00102	0.00074
30	30.9	1.43	2950			0.00074
34	34.3	1.52	3400			0.00073
37.69	38.2	1.42	3952*	2045	0.00105	0.00071
38	38.2	1.39	3900			0.00071
42	43.1	1.42	4460			0.00067
45.64	49.4	1.45	5152*	2020	0.00107	0.00063
46	49.4	1.44	5090			0.00063
50	58.3	1.42	5820			0.00062
54	69.2	0.73	6670			0.00047
58	71.0	0.00	7590			0.00044
62	71.1	0.00	8520			0.00049
66	71.1	0.00	9450			0.00038
69.70	71.1	0.00	10062*	5538	0.00035	0.00033
70	71.1	-0.01	10400			0.00033
74	71.1	0.00	11300			0.00031
78	71.1	0.00	12200			0.00032
82	71.1	0.00	13100			0.00028
85.78	71.1	0.00	13711*	9187	0.00028	0.00031
86	71.1	-0.01	14000			0.00031
90	71.0	0.00	14900			0.00029

TABLE 2

TEMPERATURE PROFILES

Run 080668-1

X = 13.78 in

y,in	y^+	t^+	u/U_∞	$\bar{t}$
0.0085	6.42	5.97	0.346	0.372
0.0105	7.93	6.66	0.386	0.415
0.0145	11.0	7.81	0.473	0.486
0.0185	14.0	8.73	0.539	0.544
0.0235	17.8	9.66	0.600	0.602
0.0295	22.3	10.4	0.646	0.650
0.0365	27.6	11.1	0.672	0.693
0.0455	34.4	11.7	0.708	0.726
0.0655	49.5	12.4	0.749	0.774
0.1055	79.7	13.3	0.792	0.828
0.1655	125.0	14.1	0.837	0.878
0.2705	204.0	15.0	0.903	0.931
0.4705	355.0	15.8	0.987	0.984
0.6705	507.0	16.1	1.000	1.000

X = 29.67 in

y,in	y^+	t^+
0.0085	7.57	6.36
0.0115	10.2	7.72
0.0155	13.8	8.98
0.0205	18.3	10.4
0.0265	23.6	11.6
0.0335	29.8	12.5
0.0425	37.8	13.4
0.0555	49.4	14.1
0.0805	71.7	14.9
0.1355	138.0	16.2
0.2555	227.0	17.2
0.4055	361.0	18.1
0.6055	539.0	18.9
0.7055	628.0	19.0

X = 37.69 in

y,in	y^+	t^+
0.0085	9.14	6.90
0.0105	11.3	7.78
0.0125	13.4	8.64
0.0155	16.7	9.84
0.0195	21.0	11.2
0.0235	25.3	12.2
0.0275	29.6	13.1
0.0325	34.9	13.8
0.0415	44.6	14.8
0.0585	62.9	16.0
0.0835	89.8	16.8
0.1285	138.0	17.7
0.2285	246.0	18.9
0.3535	380.0	19.9
0.5535	595.0	20.8
0.7535	810.0	21.0

X = 45.64 in

y,in	y^+	t^+
0.0085	11.6	8.12
0.0105	14.3	9.16
0.0145	19.7	11.2
0.0185	25.2	12.7
0.0235	32.0	14.2
0.0335	45.6	16.1
0.0435	59.2	17.2
0.0535	72.8	18.0
0.0735	100.0	18.9
0.1185	161.0	19.9
0.1685	229.0	20.7
0.2185	297.0	21.4
0.3185	433.0	22.3
0.4185	569.0	22.8
0.5685	773.0	23.2
0.6685	910.0	23.3

X = 69.70 in

y,in	y^+	t^+
0.0085	16.9	8.50
0.0105	20.9	9.39
0.0135	26.8	10.5
0.0185	36.8	11.5
0.0255	50.7	12.4
0.0355	70.6	13.2
0.0555	110.0	14.2
0.0755	150.0	14.9
0.1105	220.0	15.8
0.1605	319.0	16.8
0.2105	418.0	17.5
0.2855	568.0	18.2
0.3855	766.0	18.5
0.4855	965.0	18.6
0.5355	1064.0	18.7

X = 85.78 in

y,in	y^+	t^+
0.0085	15.8	8.64
0.0115	21.3	9.86
0.0155	28.7	11.0
0.0205	38.0	11.7
0.0305	56.6	12.5
0.0505	93.6	13.3
0.0805	149.0	14.2
0.1305	242.0	15.1
0.1805	335.0	16.0
0.2805	520.0	17.5
0.3805	705.0	18.4
0.4305	798.0	18.6
0.5805	1076.0	18.7

Run 072968-1

X = 13.78 in

y,in	y^+	t^+	u/U_∞	$\bar{t}$
0.0085	5.13	4.61	0.276	0.288
0.0125	7.54	5.63	0.365	0.352
0.0165	9.95	6.49	0.433	0.406
0.0225	13.6	7.72	0.498	0.482
0.0285	17.2	8.70	0.541	0.543
0.0375	22.6	9.63	0.593	0.601
0.0475	28.7	10.3	0.625	0.640
0.0675	40.7	11.1	0.662	0.694
0.0975	58.8	11.9	0.704	0.745
0.1475	89.0	12.8	0.752	0.799
0.2225	134.0	13.7	0.811	0.856
0.3225	195.0	14.6	0.876	0.912
0.4225	255.0	15.2	0.938	0.951
0.5725	345.0	15.8	0.990	0.986
0.7725	466.0	16.0	1.000	0.998
0.8725	526.0	16.0	1.000	1.000

X = 29.67 in

y,in	y^+	t^+
0.0085	6.48	5.65
0.0115	8.77	6.79
0.0155	11.8	8.14
0.0195	14.9	9.31
0.0255	19.5	10.7
0.0325	24.8	11.8
0.0435	33.2	12.9
0.0635	48.4	14.1
0.0985	75.1	15.4
0.1485	113.0	16.5
0.2235	171.0	17.7
0.3235	247.0	18.8
0.4235	323.0	19.7
0.5735	438.0	20.7
0.7735	590.0	21.4

X = 37.69 in

y,in	y^+	t^+
0.0085	8.07	6.82
0.0125	11.9	8.58
0.0165	15.7	10.1
0.0215	20.4	11.5
0.0285	27.1	12.8
0.0385	36.6	14.1
0.0535	50.8	15.2
0.0835	79.3	16.5
0.1335	127.0	18.0
0.1835	174.0	19.1
0.2585	245.0	20.3
0.3585	340.0	21.4
0.4585	435.0	22.4
0.6586	625.0	23.6
0.8585	815.0	23.8

X = 45.64 in

y,in	y^+	t^+
0.0085	10.3	7.39
0.0125	15.2	9.26
0.0165	20.0	10.9
0.0225	27.3	12.4
0.0325	39.4	13.8
0.0425	51.5	14.7
0.0625	75.8	15.9
0.0925	112.0	17.3
0.1425	173.0	18.8
0.1925	233.0	20.1
0.2675	324.0	21.6
0.3675	445.0	22.9
0.4675	567.0	23.8
0.6675	809.0	24.7
0.7675	930.0	24.8

X = 69.70 in

y,in	y^+	t^+
0.0085	13.2	7.55
0.0125	19.4	9.34
0.0165	25.6	10.3
0.0225	35.0	11.2
0.0315	49.0	12.0
0.0565	87.8	13.3
0.1015	158.0	14.7
0.1515	235.0	16.0
0.2265	352.0	17.7
0.3265	507.0	19.9
0.4265	663.0	22.0
0.5265	818.0	23.0
0.6265	973.0	23.4
0.7265	1129.0	23.5

X = 85.78 in

y,in	y^+	t^+
0.0085	12.7	7.53
0.0115	17.2	8.81
0.0165	24.7	10.1
0.0225	33.6	11.0
0.0325	48.6	11.9
0.0525	78.5	12.9
0.1025	153.0	14.3
0.1525	228.0	15.3
0.2275	340.0	16.6
0.3275	490.0	18.0
0.4275	639.0	19.5
0.5275	789.0	20.9
0.6275	938.0	22.3
0.7275	1088.0	23.1
0.8275	1237.0	23.4

TABLE 2 (continued)

Run 082768-1

X = 13.78 in

y,in	y^+	t^+	u/U_∞	$\bar{t}$
0.0085	3.21	3.83	0.151	0.137
0.0125	4.71	5.10	0.229	0.183
0.0215	8.11	7.72	0.278	0.277
0.0315	11.9	9.66	0.346	0.347
0.0465	17.5	11.4	0.381	0.408
0.0715	27.0	13.2	0.437	0.473
0.1065	40.2	14.8	0.487	0.530
0.1565	59.0	16.4	0.536	0.589
0.2065	77.9	17.8	0.586	0.639
0.2815	106.0	19.7	0.655	0.707
0.3815	144.0	21.6	0.741	0.776
0.4815	182.0	23.4	0.813	0.839
0.6815	257.0	26.3	0.945	0.943
0.8815	332.0	27.7	0.994	0.994
1.0315	389.0	27.9	1.000	1.000

X = 29.67 in

y,in	y^+	t^+
0.0085	4.41	4.94
0.0125	6.48	6.69
0.0225	11.7	10.4
0.0325	16.9	12.6
0.0425	22.0	14.3
0.0625	32.4	16.2
0.1075	55.7	19.3
0.1575	81.6	21.8
0.2325	121.0	24.3
0.3325	172.0	27.4
0.4325	224.0	29.9
0.5825	302.0	33.2
0.7825	406.0	36.7
0.9825	509.0	39.5
1.1825	613.0	40.5

X = 37.69 in

y,in	y^+	t^+
0.0085	5.54	5.97
0.0125	8.15	7.93
0.0215	14.0	11.2
0.0315	20.5	13.5
0.0465	30.3	15.8
0.0765	49.9	18.9
0.1265	82.5	22.1
0.1765	115.0	24.6
0.2765	180.0	28.7
0.3765	245.0	32.2
0.4765	311.0	35.4
0.6765	441.0	40.2
0.8765	572.0	44.1
1.0765	702.0	45.9
1.2765	832.0	46.3

X = 45.64 in

y,in	y^+	t^+
0.0095	8.08	6.55
0.0135	11.5	9.06
0.0235	20.0	12.3
0.0385	32.8	15.1
0.0685	58.3	18.6
0.1185	101.0	22.5
0.1685	143.0	25.7
0.2685	228.0	30.7
0.3685	313.0	35.4
0.4685	399.0	39.4
0.6685	569.0	45.6
0.8685	739.0	49.6
1.0685	909.0	51.0
1.1185	951.0	51.1

X = 69.70 in

y,in	y^+	t^+
0.0085	5.93	7.34
0.0125	8.72	9.30
0.0175	12.2	10.7
0.0245	17.1	12.2
0.0335	23.4	13.5
0.0465	31.7	14.8
0.0635	44.3	16.2
0.0885	61.7	17.7
0.1335	93.1	20.1
0.1835	128.0	21.9
0.2585	180.0	24.7
0.4085	285.0	29.9
0.6085	424.0	37.8
0.8085	564.0	46.6
1.0085	703.0	54.7
1.2085	843.0	57.8
1.4085	982.0	58.4

X = 85.78 in

y,in	y^+	t^+
0.0095	5.92	6.97
0.0175	10.9	10.0
0.0325	20.3	12.8
0.0625	39.0	15.5
0.1125	70.2	18.5
0.1625	101.0	20.4
0.2375	148.0	22.7
0.3375	210.0	25.5
0.4875	304.0	28.8
0.6875	429.0	33.7
0.8875	553.0	38.5
1.0875	678.0	43.9
1.2875	803.0	50.0
1.4875	928.0	55.8
1.6875	1052.0	58.8
1.8875	1177.0	59.7
2.0875	1302.0	59.8

LIST OF FIGURES

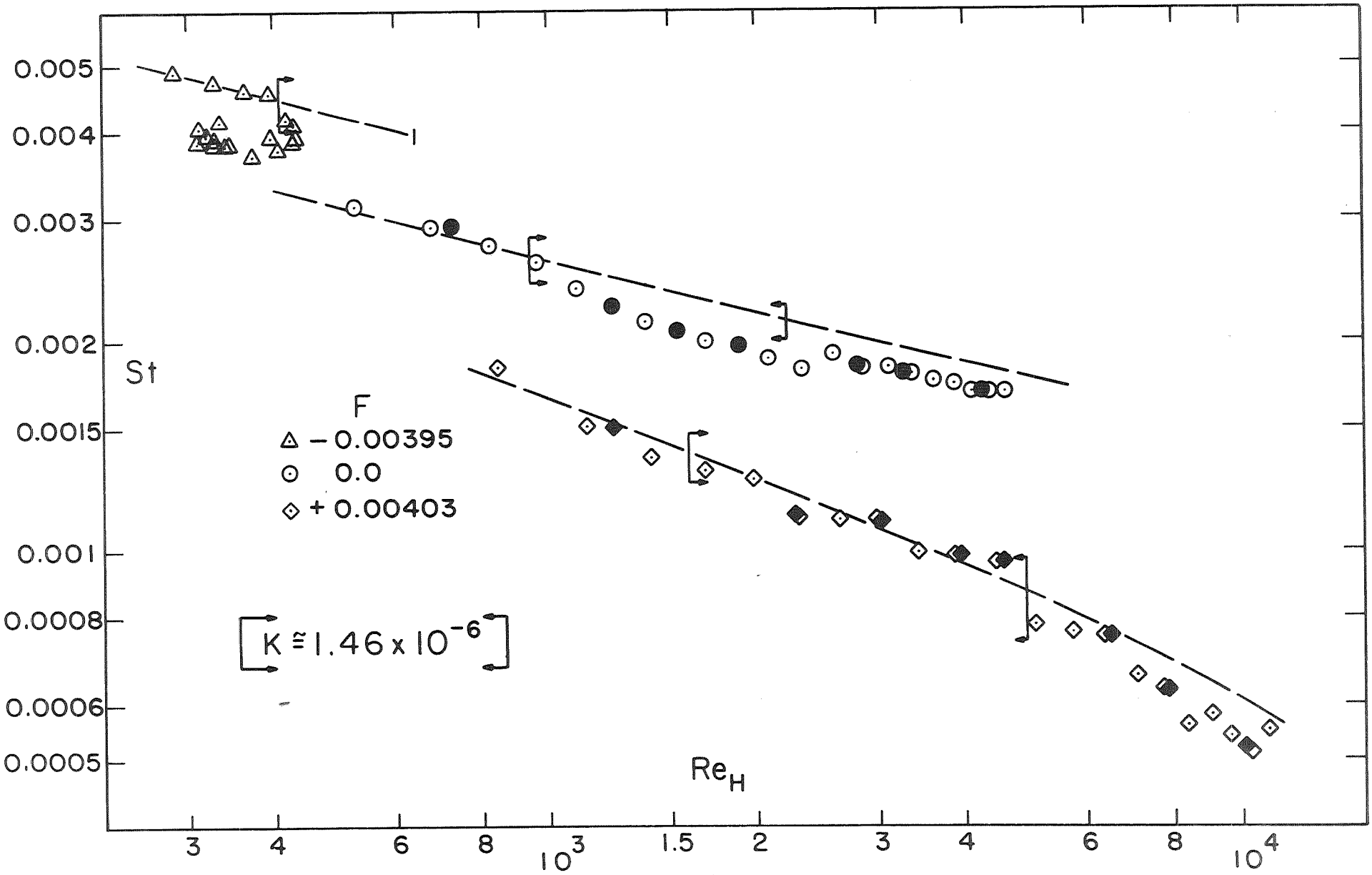

Figure 1. Local heat transfer results for transpiration and acceleration

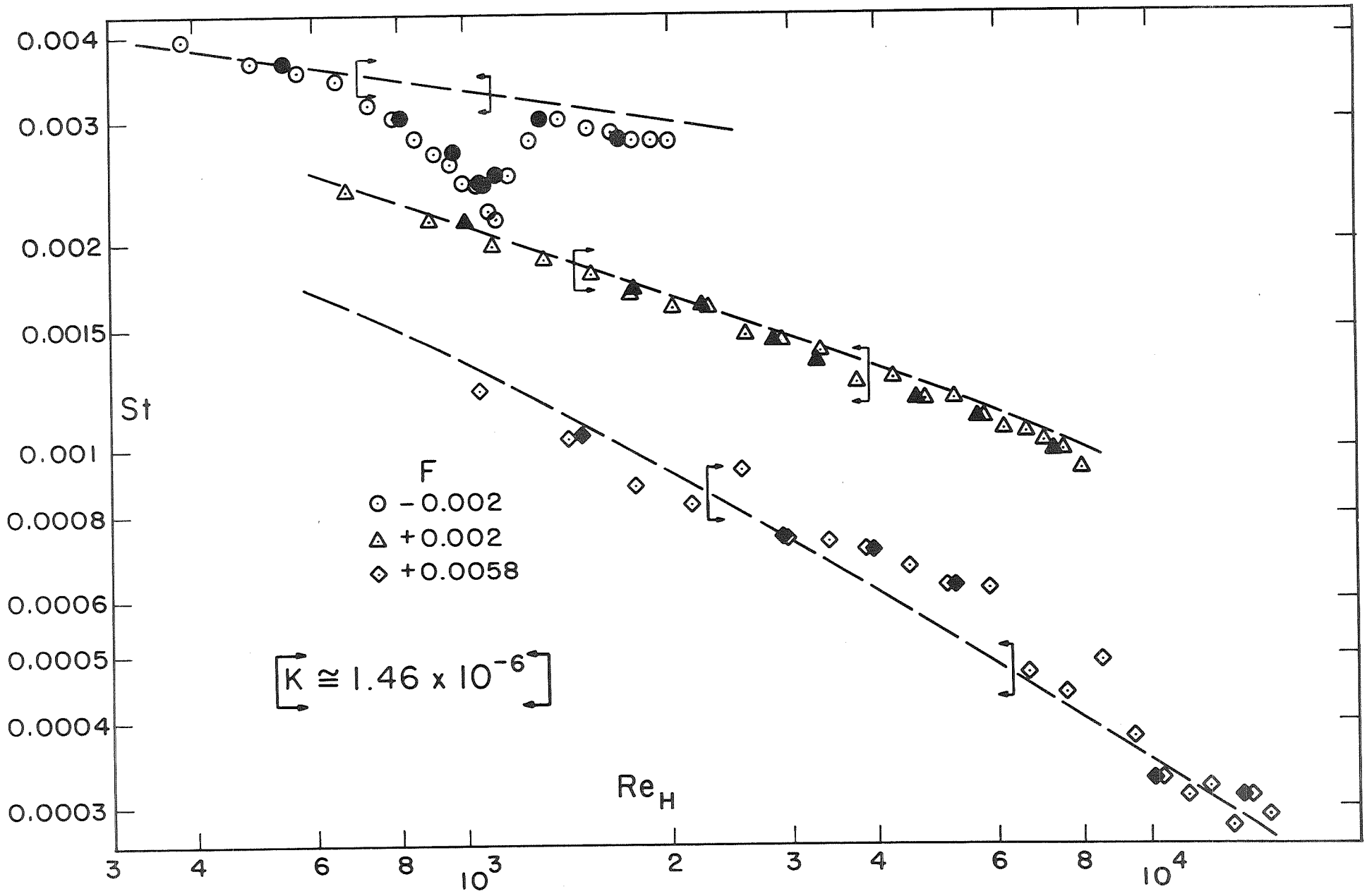

Figure 2. Local heat transfer results for transpiration and acceleration

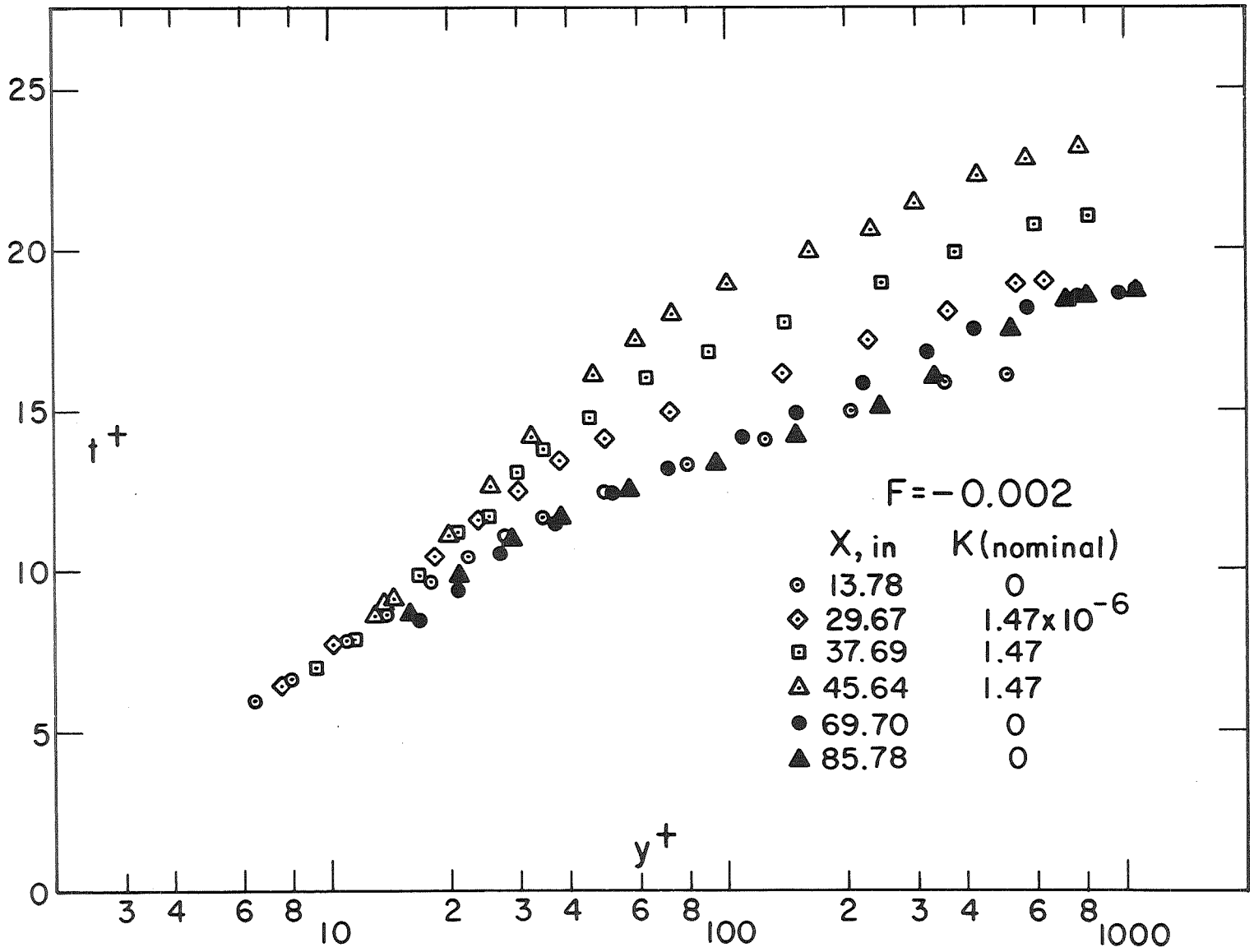

Figure 3. Temperature profiles for F = -0.002

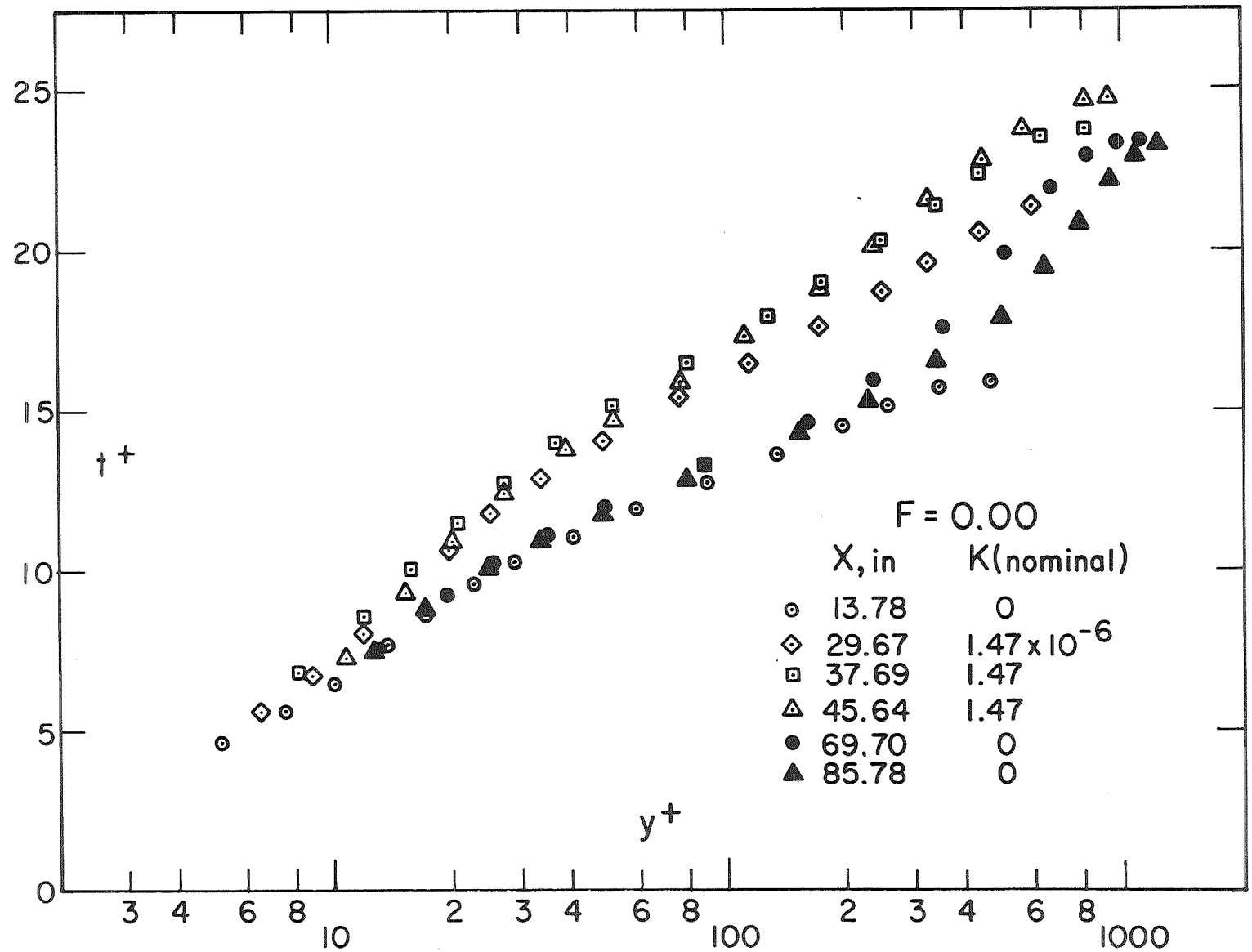

Figure 4. Temperature profiles for F = 0.0

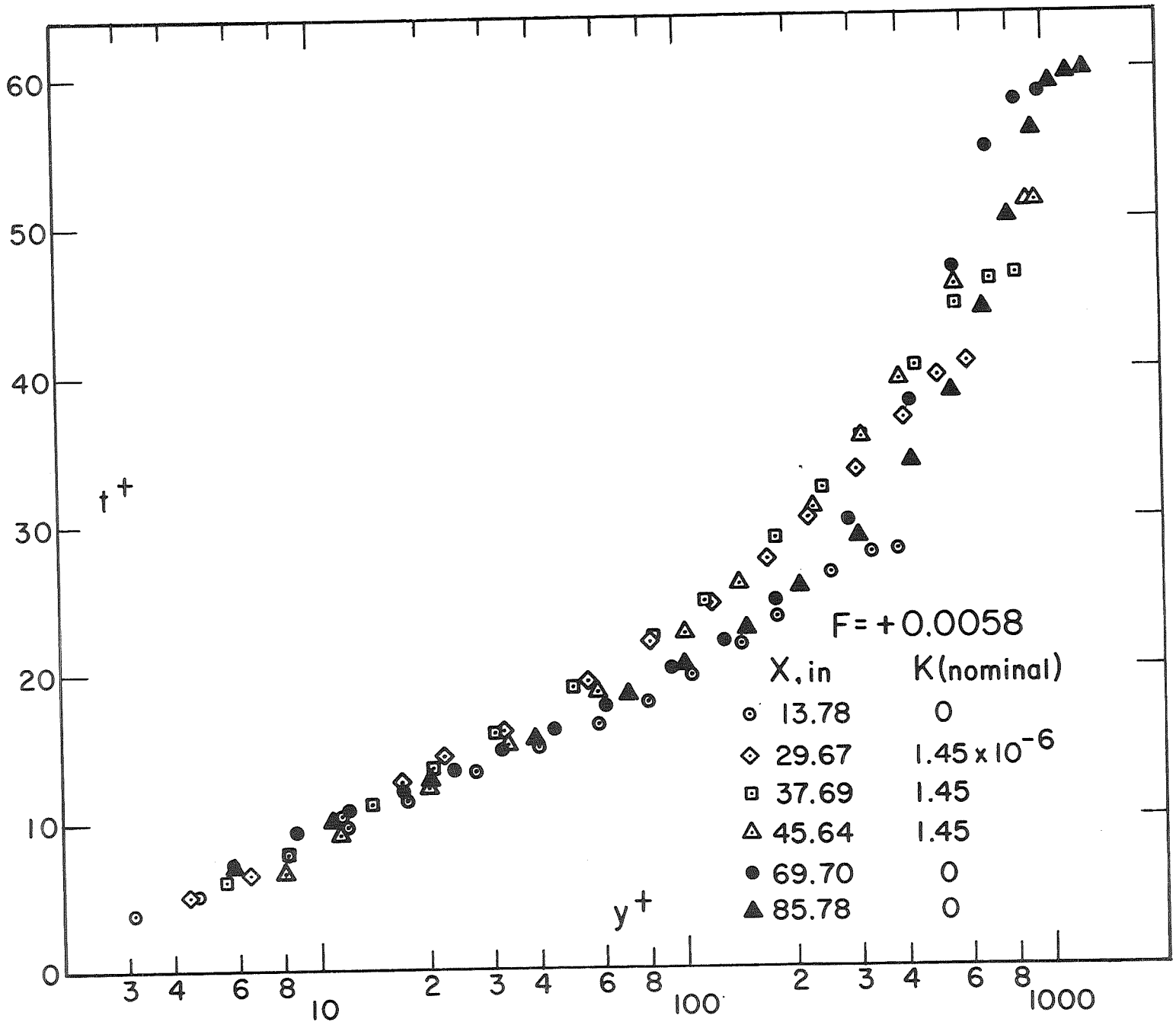

Figure 5. Temperature profiles for F = +0.0058